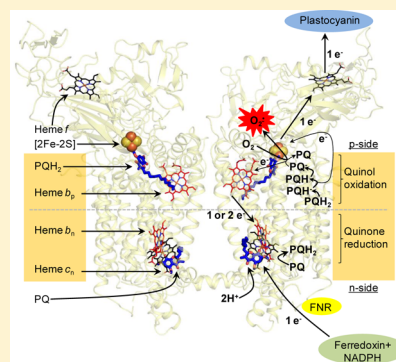


# Mechanism of Enhanced Superoxide Production in the Cytochrome $b_6f$ Complex of Oxygenic Photosynthesis

Danas Baniulis,<sup>§,†</sup> S. Saif Hasan,<sup>§</sup> Jason T. Stofleth,<sup>‡</sup> and William A. Cramer\*

Department of Biological Sciences, Hockmeyer Hall of Structural Biology, Purdue University, West Lafayette, Indiana 47907, United States

**ABSTRACT:** The specific rate of superoxide ( $O_2^{\bullet-}$ ) production in the purified active crystallizable cytochrome  $b_6f$  complex, normalized to the rate of electron transport, has been found to be more than an order of magnitude greater than that measured in isolated yeast respiratory  $bc_1$  complex. The biochemical and structural basis for the enhanced production of  $O_2^{\bullet-}$  in the cytochrome  $b_6f$  complex compared to that in the  $bc_1$  complex is discussed. The higher rate of superoxide production in the  $b_6f$  complex could be a consequence of an increased residence time of plastoquinone/plastoquinol in its binding niche near the Rieske protein iron–sulfur cluster, resulting from (i) occlusion of the quinone portal by the phytyl chain of the unique bound chlorophyll, (ii) an altered environment of the proton-accepting glutamate believed to be a proton acceptor from semiquinone, or (iii) a more negative redox potential of the heme  $b_p$  on the electrochemically positive side of the complex. The enhanced rate of superoxide production in the  $b_6f$  complex is physiologically significant as the chloroplast-generated reactive oxygen species (ROS) functions in the regulation of excess excitation energy, is a source of oxidative damage inflicted during photosynthetic reactions, and is a major source of ROS in plant cells. Altered levels of ROS production are believed to convey redox signaling from the organelle to the cytosol and nucleus.



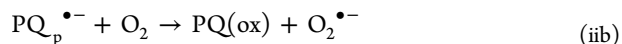
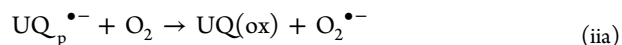
The protein subunits and prosthetic groups in the structure from the cyanobacterium *Mastigocladus laminosus*<sup>1</sup> are shown in Figure 1. The role of the cytochrome  $bc_1$  complex in the generation of  $O_2^{\bullet-}$  by the mitochondrial respiratory electron transport pathway has been described and reviewed.<sup>2–8</sup> By analogy with the  $bc_1$  complex, the site of production of superoxide in the cytochrome  $b_6f$  complex is shown in Figure 2, with an emphasis on the electrochemically positive (p, lumen)-side plastoquinone/plastoquinol binding site that, by analogy with the mechanism proposed for the  $bc_1$  complex, is close to the site of oxygen reduction by plastoquinone and resulting superoxide formation. The production of reactive oxygen species (ROS) in chloroplasts not only underlies oxidative damage inflicted in photosynthetic electron transport<sup>9</sup> but also functions in redox signaling from the organelle to the cytosol and nucleus,<sup>10</sup> and in the regulation and dissipation of excess excitation energy.<sup>11</sup> Although the production of  $O_2^{\bullet-}$  by the cytochrome  $b_6f$  complex of oxygenic photosynthesis has been detected by EPR spectroscopy,<sup>12</sup> details about rates and constraints have not yet been published. This study provides quantitative information about the level of  $O_2^{\bullet-}$  generated in electron transport through the  $b_6f$  complex that mediates these signaling processes.

$O_2^{\bullet-}$  can be formed through a one-electron reduction of the oxygen molecule, with a midpoint redox potential of  $-0.14$  V in the aqueous phase.<sup>13,14</sup>

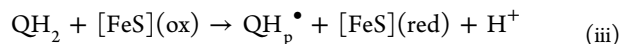


Ubisemiquinone,  $UQ_p^{\bullet-}$ , formed on the electrochemically positive, p-side, of the complex (reaction iia), is a reductant for

oxygen proximal to the  $bc_1$  complex in mitochondrial and photosynthetic bacterial membranes. Because ubisemiquinol is a reductant of low-potential heme  $b_p$  in the  $bc_1$  complex,<sup>15</sup> it has been inferred that the ubisemiquinone formed in the  $bc_1$  complex through quinol oxidation by the high-potential segment of the electron transport chain has a sufficiently reducing potential to form superoxide,  $O_2^{\bullet-}$  (reaction iia). On the basis of the similarity of the crystal structures of the protein core<sup>16</sup> and of the midpoint redox potentials [ $E_{m7}$  values of 80 mV (plastoquinone/quinol)<sup>17</sup> and 60 mV (ubiquinone/quinol)<sup>18</sup>], it is inferred that plastoquinone,  $PQ_p^{\bullet-}$ , can serve as the reductant for the generation of superoxide in the  $b_6f$  complex (Figure 2B and reaction iib):



The p-side semiquinone,  $Q_p^{\bullet-}$ , is generated through the one-electron oxidation of ubiquinol or plastoquinol,  $QH_2$ , by the [FeS] cluster of the high-potential Rieske iron–sulfur protein subunit of the complex:



$QH_p^{\bullet-}$  generated in reaction iii transfers a proton to the p-side aqueous phase through an intraprotein pathway in the

Received: October 1, 2013

Revised: December 1, 2013

Published: December 3, 2013



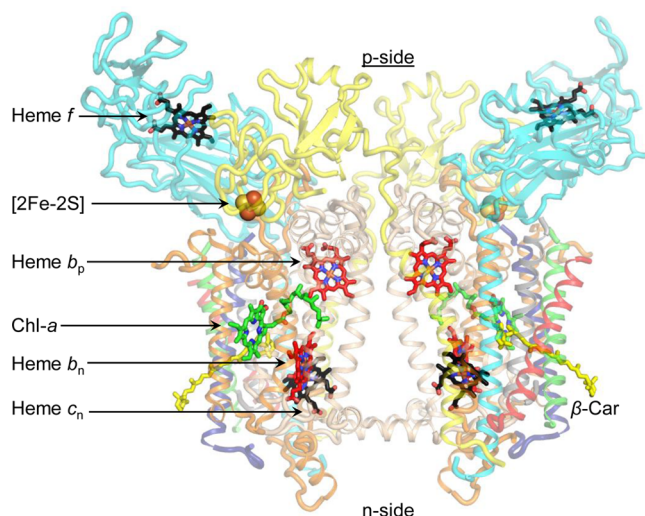


**Figure 1.** Dimeric cytochrome  $b_6f$  complex (PDB entry 4H44). Prosthetic groups in the cytochrome  $b_6f$  complex. Hemes  $b_p$  (red),  $b_n$  (red), and  $c_n$  (black) are redox-active prosthetic groups located within the transmembrane domain and constitute the low-potential chain. Heme  $f$  (black) and the [2Fe-2S] cluster (orange and yellow spheres) form the high-potential chain and are associated with the p-side extrinsic domains of cytochrome  $f$  and ISP, respectively. A chlorophyll  $a$  (green) and a  $\beta$ -carotene (yellow) are also associated with the complex. Polypeptides are shown as ribbons. Color code: cytochrome  $b_6$  (cyt  $b_6$ ), wheat; subunit IV (subIV), orange; cytochrome  $f$  (cyt  $f$ ), cyan; iron-sulfur protein (ISP), yellow; PetL, red; PetM, green; PetG, blue; PetN, gray.

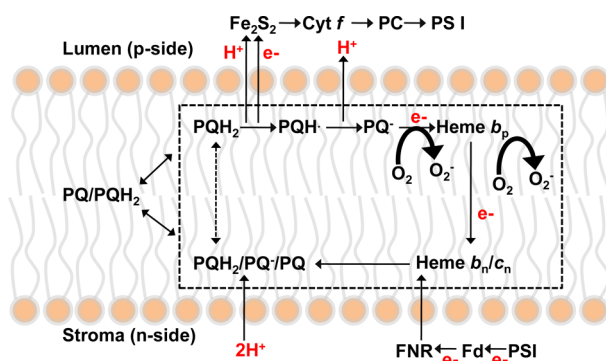
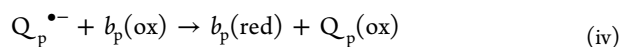


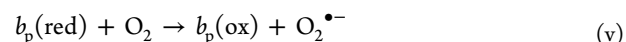
**Figure 2.** Transmembrane electron transfer and Q-cycle pathway in a schematic of the charge transfer reactions in the cytochrome  $b_6f$  complex, indicating the branching of electrons from the anionic semiquinone reductant,  $PQ_p^{\bullet-}$ , and heme  $b_p$  to  $O_2$ . The latter reactions are responsible for the formation of superoxide,  $O_2^{\bullet-}$ .

cytochrome  $bc_1$  complex.<sup>19</sup> A similar p-side proton release pathway, which forms the p-side anionic plastoquinone,  $PQ_p^{\bullet-}$ , has recently been defined by crystallographic analysis of the cytochrome  $b_6f$  complex.<sup>20</sup>

In a Q-cycle mechanism,<sup>15,21–24</sup> an electron is transferred from the deprotonated  $Q_p^{\bullet-}$  to p-side heme  $b_p$  (reaction iv) and then across the hydrophobic domain of the membrane through the n-side heme,  $b_n$ , to reduce quinone specifically bound on the n-side of the complex.



Reduced heme  $b_p$  may be an alternative source of electrons for the reduction of  $O_2$  to  $O_2^{\bullet-}$ .<sup>25</sup>



It has been inferred<sup>2,8</sup> that superoxide production in the cytochrome  $bc_1$  complex occurs as a bypass of reaction iv above of the Q-cycle by reaction iia, b, or v, the latter reaction having been suggested as being dominant.<sup>4,25</sup> The participation of reactions iib and v in superoxide generation in the cytochrome  $b_6f$  complex is shown in the Q-cycle scheme (Figure 2). The n-side ubiquinone reduction in the  $bc_1$  complex is blocked by the quinone analogue inhibitor antimycin A, which occupies the n-side quinone binding site with high affinity.<sup>26</sup> A consequence of this inhibition of the transmembrane electron transfer chain would be accumulation of the p-side semiquinone electron donor,  $Q_p^{\bullet-}$  (reaction iv). The probability of electron transfer through the other branch of the  $Q_p^{\bullet-}$  oxidation pathway that forms superoxide (reaction iia) would then be increased. Thus, the specific n-side quinone analogue inhibitor, antimycin A, causes a large increase in the specific rate of formation of  $O_2^{\bullet-}$ , relative to the electron transport rate, by the  $bc_1$  complex of yeast or bovine mitochondria,<sup>4,7,8,27,28</sup> and the photosynthetic bacterium, *Rhodospirillum rubrum*.<sup>29</sup> No n-side inhibitor comparable in efficacy to that of antimycin has been found for the  $b_6f$  complex, because the unique heme  $c_n$  occupies the quinone binding site homologous to that of antimycin,<sup>30</sup> which results in an altered binding interaction of an n-side quinone analogue inhibitor.<sup>31</sup> Although the quinone analogue inhibitor NQNO binds specifically to n-side heme  $c_n$ <sup>1</sup> and inhibits the oxidation of heme  $b_n$ ,<sup>32–34</sup> unlike the inhibition of the respiratory chain resulting from the action of antimycin, the extent of inhibition of linear electron transport, by NQNO, is low.<sup>32</sup>

It has been proposed that  $O_2^{\bullet-}$  production occurs in the cytochrome  $b_6f$  complex<sup>2</sup> by a mechanism (reaction iib) similar to the alternative pathway for the  $bc_1$  complex (reaction iia).<sup>2,3,5,8</sup> However, experimental details about the rate of  $O_2^{\bullet-}$  generation in the  $b_6f$  and  $bc_1$  complexes have not been described. This study compares the specific rate of  $O_2^{\bullet-}$  generation in cytochrome  $b_6f$  and  $bc_1$  complexes and proposes that the level of  $O_2^{\bullet-}$  production by the  $b_6f$  and  $bc_1$  complexes is dependent upon the residence time of reduced quinone species within the  $Q_p$  portal.

## MATERIALS AND METHODS

**Materials.** ADPH and  $H_2O_2$  were purchased from Anaspec (Fremont, CA), equine heart cytochrome  $c$ , HRP and SOD enzymes, decyl-ubiquinol, and decyl-plastoquinol from Sigma-Aldrich (St. Louis, MO), DDM and UDM from Antrace (Maumee, OH), and other reagents from Mallinckrodt/Baker, Inc. (Phillipsburg, NJ).

**Preparation of the Yeast Mitochondrial Cytochrome  $bc_1$  Complex.** The cytochrome  $bc_1$  complex from yeast was purified in the laboratory of B. L. Trumpower, as previously described.<sup>28</sup>

**Preparation of Thylakoid Membranes and Purification of the Cytochrome  $b_6f$  Complex.** Cyanobacterial thylakoid membranes and the  $b_6f$  complex were prepared and purified, respectively, as described previously,<sup>35</sup> as were spinach chloroplast thylakoid membranes and the cytochrome  $b_6f$  complex.<sup>35,36</sup> Membranes were resuspended (chlorophyll  $a$  concentration of 2 mg/mL) in TNE [30 mM Tris-HCl (pH 7.5), 50 mM NaCl, 1 mM EDTA, and 0.3 M sucrose, with protease inhibitors benzamidine (2 mM) and  $\epsilon$ -aminocaproic acid (2 mM)].

**Purification of Plastocyanin.** Plastocyanin from *Nostoc*<sup>36</sup> and spinach<sup>37</sup> was purified as described previously, and for the latter, a modified procedure included size exclusion and anion-exchange chromatography.

**Activities for ubiquinol-cytochrome *c* and plasto-quinol-plastocyanin oxidoreductase** were assayed with the purified *bc*<sub>1</sub> and *b<sub>6</sub>f* complexes, respectively. For the *bc*<sub>1</sub> complex, the assay mixture contained 50 μM equine heart cyt *c*, 50 mM MOPS (pH 6.9), 0.4 mM DDM, 1 mM KCN, and 0.05 mM decyl-ubiquinol. Reduction of cyt *c*, initiated by addition of 5 or 45 nM cytochrome *bc*<sub>1</sub> for uninhibited or inhibited activity, respectively, was monitored through the change in absorbance at 551 nm, and the activity was based on an extinction coefficient of  $2.1 \times 10^4 \text{ M}^{-1} \text{ cm}^{-1}$ .<sup>38</sup> For the plastoquinol-plastocyanin oxidoreductase activity of the *b<sub>6</sub>f* complex or thylakoid membranes, the assay mixture contained plastocyanin ( $10^{-2} \text{ M}$ ) from *Nostoc* or spinach, 50 mM Tris-HCl (pH 7.5), 1 mM UDM, and 20 μM decyl-plastoquinol. Changes in absorbance were assayed on a Cary 4000 spectrophotometer. The reaction was initiated by addition of 5 nM cyt *b<sub>6</sub>f* complex or 3 μM Chl *a* equivalent of thylakoid membranes, and activity was monitored as the change in plastocyanin absorbance at 597 nm ( $\epsilon_{\text{mM}} = 4.9 \text{ mM}^{-1} \text{ cm}^{-1}$ ).<sup>39</sup> Inhibitors were added as ethanol stocks (<0.5% of the total reaction volume). Initial electron transport rates were determined using the SLOPE function in the support software of a Cary 4000 spectrophotometer and calculated as moles of electrons transferred per mole of *bc* complex per second, or per  $10^3$  moles of Chl *a* equivalent of thylakoid membranes.

**Superoxide Production Assay.** The amount of superoxide released from cytochrome *bc* complexes was measured fluorometrically via the formation of  $\text{H}_2\text{O}_2$ . In the presence of saturating levels of SOD, superoxide released from cytochrome *bc* complexes is converted to  $\text{H}_2\text{O}_2$ . ADPH reacts with  $\text{H}_2\text{O}_2$  in a 1:1 stoichiometry, in the presence of HRP as a catalyst, to produce the fluorescent oxidation product resorufin. The reaction mixture contained for the yeast *bc*<sub>1</sub> complex 50 mM MOPS (pH 6.9), 0.4 mM DDM, 50 μM ADHP, 1 unit/mL HRP, 50 μM equine heart cyt *c*, and 50 μM decyl-ubiquinol and for the *b<sub>6</sub>f* complex 50 mM MOPS (pH 6.9), 1 mM UDM, 40 μM ADHP, 20 μM decyl-plastoquinol, 1 unit/mL HRP, 300 units/mL SOD, and plastocyanin (10 mM) from *Nostoc* or spinach or 25 μM cyt *c* from equine heart. Inhibitors were added as ethanol stocks (<0.5% of the total reaction volume). The reaction was started by adding the *bc*<sub>1</sub> complex to a final concentration of 5 or 45 nM for the measurement of uninhibited or inhibited activity, respectively, or the *b<sub>6</sub>f* complex to a final concentration of 5 nM (3 μM Chl *a* equivalent of thylakoid membranes). The fluorescence indicator of superoxide production was measured by excitation and emission at 530 nm (2 nm bandwidth) and 590 nm (1 nm bandwidth), respectively, utilizing a FluoroMax-3 fluorimeter (Horiba Jobin Yvon Inc., Edison, NJ) and calibrated using  $\text{H}_2\text{O}_2$  standards. The initial rate of superoxide production was estimated using the LINEST function of MS Office Excel and calculated as moles of superoxide generated per second per mole of *bc* complex, or per  $10^3$  moles of Chl *a* equivalent of thylakoid membranes.

**Sequence alignment** was performed with Clustal-Omega using default parameters.<sup>40,41</sup> The following cytochrome *b<sub>6</sub>* polypeptide sequences were obtained from the NCBI database: *Synechocystis* sp. PCC 6803, BAA10149.1; *Synechococcus elongatus* PCC 6301, BAD79961.1; *Nostoc* sp. PCC 7120,

BAB75120.1; *M. laminosus*, AAR26242.1; *Chlamydomonas reinhardtii*, CAA44690.1; *Arabidopsis thaliana*, NP\_051088.1; *Spinacea oleracea*, CAA30128.1.

Panels A and B of Figure 4 were generated with Pymol (<http://www.pymol.org>), from structural superposition of cytochrome *bc*<sub>1</sub> complex crystal structures (PDB entries 1NTZ<sup>42</sup> and 3CX5<sup>43</sup>) and cytochrome *b<sub>6</sub>f* complex crystal structures (PDB entries 4H44 and 4H13<sup>20</sup>).

## RESULTS

**Superoxide Production in the Cytochrome *bc*<sub>1</sub> Complex.** The rate of superoxide ( $\text{O}_2^{\bullet-}$ ) production in the yeast mitochondrial *bc*<sub>1</sub> complex, using decyl-ubiquinol as the electron donor, is 0.1–0.2% of the electron transport rate (Table 1), a value similar to results in the literature obtained

**Table 1. Production of Superoxide by the Cytochrome *bc*<sub>1</sub> Complex from Yeast Mitochondria**

	electron transfer rate (cyt <i>bc</i> <sub>1</sub> <sup>-1</sup> s <sup>-1</sup> )	superoxide production rate (cyt <i>bc</i> <sub>1</sub> <sup>-1</sup> s <sup>-1</sup> )	superoxide production (% of electron transfer rate)
control, no inhibitor <sup>a</sup>	151 ± 6.1 (n = 5)	0.21 ± 0.13 (n = 8)	0.14 ± 0.06
antimycin A, 20 μM	1.2 ± 0.1 (n = 4)	0.13 ± 0.03 (n = 6)	10.6 ± 2.3
DBMIB, 2 μM	28.3 ± 3.1 (n = 4)	0.04 ± 0.01 (n = 3)	0.14 ± 0.02

<sup>a</sup>For reactions in the absence and presence of inhibitor, the *bc*<sub>1</sub> complex was used at concentrations of 5 and 45 nM, respectively, with cytochrome *c* as the electron acceptor. *n* is the number of trials.

with the *bc*<sub>1</sub> complex from yeast mitochondria.<sup>5,7,8,44</sup> This is approximately the same rate, essentially a background rate, that was obtained in the presence of the p-side quinone analogue inhibitor DBMIB (Table 1), which prevents quinol oxidation by the [2Fe-2S] cluster.<sup>45</sup> Higher rates have been reported for mitochondrial *bc*<sub>1</sub> complexes, on the basis of a difference in measurements with and without superoxide dismutase to assay  $\text{O}_2^{\bullet-}$  production.<sup>44</sup>  $\text{O}_2^{\bullet-}$  generation has also been measured with the *bc*<sub>1</sub> complex obtained from the purple photosynthetic bacterium *Rb. sphaeroides*,<sup>29,46</sup> for which the rate of  $\text{O}_2^{\bullet-}$  production relative to the electron transport rate was not reported. In our experiments with the yeast *bc*<sub>1</sub> complex, the specific rate of  $\text{O}_2^{\bullet-}$  production, normalized to the electron transport rate, is, however, increased greatly (>40-fold) in the presence of antimycin A (Table 1), in qualitative agreement with data obtained previously for the *bc*<sub>1</sub> complex.<sup>4,5,8,27–29</sup> The electron transport rate of the isolated *b<sub>6</sub>f* complex or membranes from spinach and *M. laminosus* and the  $\text{O}_2^{\bullet-}$  generation rate were measured by the rate of reduction of plastocyanin and by the rate of change of fluorescence emission intensity from the resorufin product of ADHP and  $\text{H}_2\text{O}_2$ , respectively (Materials and Methods). Rates of electron transport (Figure 3A) and  $\text{O}_2^{\bullet-}$  production (Figure 3B) obtained with the yeast *bc*<sub>1</sub> complex and the *b<sub>6</sub>f* complex from spinach thylakoids and *M. laminosus* are shown, from which electron transport rates were derived for the yeast *bc*<sub>1</sub> complex (Table 1), the purified *b<sub>6</sub>f* complex isolated from spinach thylakoid membranes (Table 2), the isolated *M. laminosus* cyanobacterial *b<sub>6</sub>f* complex (Table 3), and membranes of *M. laminosus* (Table 4). The rate of production of  $\text{O}_2^{\bullet-}$  by electron transfer from the decyl-plastoquinol electron donor to the *b<sub>6</sub>f* complex (Table 2) is considerably higher, a factor of 10–20,



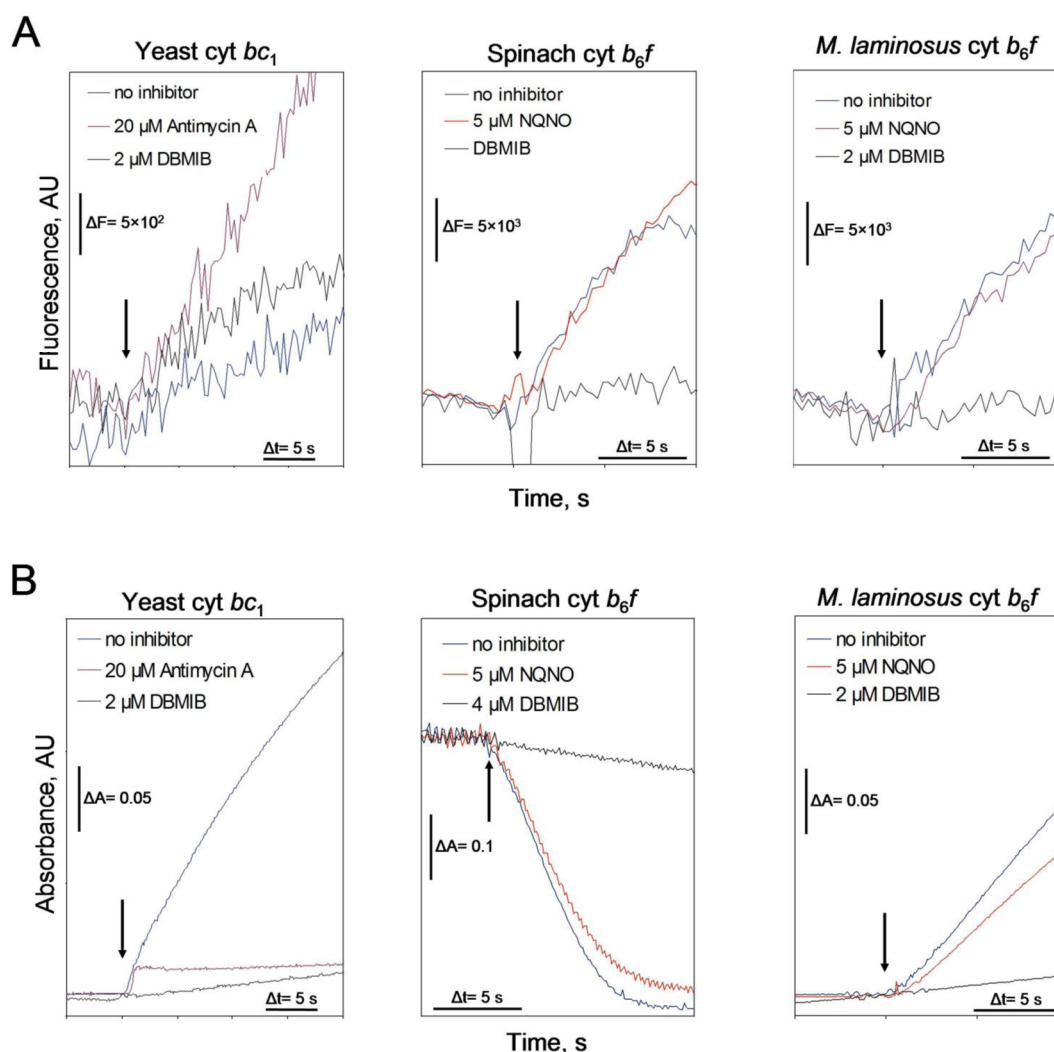


**Figure 3.** Representative original data traces for determination of rates of (A) superoxide generation and (B) electron transfer in isolated  $bc_1$  and  $b_6f$  complexes. The electron transfer and superoxide generation activities were measured as described in Materials and Methods using cytochrome  $c$  as the electron acceptor for yeast  $bc_1$ ,  $cyt\ b_6f$  from *M. lamosus*, and cyanobacterial plastocyanin for the  $b_6f$  complex from spinach. Traces are averages of two to four measurements. The background fluorescence change measured for the reaction mixture before the addition of the enzyme was subtracted from the superoxide generation activity data (B). The arrow indicates addition of 5 and 45 nM  $bc_1$  complex for reactions in the absence and presence of inhibitor, respectively, and 5 nM  $b_6f$  complex.

**Table 2. Production of Superoxide by the Isolated Spinach Cytochrome  $b_6f$  Complex with Plastocyanin as the Electron Acceptor**

	electron transfer rate <sup>a</sup> ( $cyt\ b_6f^{-1}\ s^{-1}$ )	superoxide production rate <sup>a</sup> ( $cyt\ b_6f^{-1}\ s^{-1}$ )	superoxide production rate <sup>a</sup> (% of electron transfer rate)
control, no inhibitor ( $n = 10$ )	$245 \pm 25$	$4.5 \pm 0.6$ ( $n = 10$ )	$1.9 \pm 0.3$
NQNO, 5 $\mu$ M	$196 \pm 7$ ( $n = 3$ )	$3.5 \pm 0.4$ ( $n = 3$ )	$1.8 \pm 0.2$
DBMIB, 4 $\mu$ M	nd ( $n = 4$ )	nd ( $n = 3$ )	—

<sup>a</sup> $n$  is the number of trials. “nd” indicates that the rate was too low to allow an accurate determination.

than that measured for the mitochondrial  $bc_1$  complex (Table 1). Similar results were obtained with the  $b_6f$  complex purified from the cyanobacterium *M. lamosus* using cyanobacterial plastocyanin (Table 3). Using intact membranes from *M. lamosus* (Table 4), the specific rate of superoxide production

**Table 3. Production of Superoxide by the Isolated Cytochrome  $b_6f$  Complex from the Cyanobacterium *M. lamosus* with Cyanobacterial Plastocyanin as the Electron Acceptor**

	electron transfer rate <sup>a</sup> ( $cyt\ b_6f^{-1}\ s^{-1}$ )	superoxide production rate <sup>a</sup> ( $cyt\ b_6f^{-1}\ s^{-1}$ )	superoxide production rate <sup>a</sup> (% of electron transfer rate)
control, no inhibitor ( $n = 2$ )	292	6.3 ( $n = 2$ )	2.2 ( $n = 2$ )
NQNO, 5 $\mu$ M	174 ( $n = 1$ )	2.3 ( $n = 1$ )	2.2 ( $n = 1$ )
DBMIB, 2 $\mu$ M	$6.5 \pm 1.0$ ( $n = 3$ )	nd ( $n = 6$ )	—
DBMIB, 5 $\mu$ M	$0.5 \pm 0.7$ ( $n = 3$ )	nd ( $n = 4$ )	—

<sup>a</sup> $n$  is the number of trials. “nd” indicates not determined.

by the  $b_6f$  complex is higher than that measured in the isolated  $bc_1$  complex by approximately 1 order of magnitude, but for reasons not understood, this rate is somewhat smaller than that measured with the isolated  $bc_1$  complex (Table 1).

**Table 4. Production of Superoxide by the Cytochrome  $b_6f$  Complex in Thylakoid Membranes from the Cyanobacterium *M. laminosus* with Cytochrome  $c$  as the Electron Acceptor**

	electron transfer rate <sup>a</sup> ( $\times 10^3$ chl $a^{-1}$ s $^{-1}$ )	superoxide production rate <sup>a</sup> ( $\times 10^3$ chl $a^{-1}$ s $^{-1}$ )	superoxide production rate (% of electron transfer rate)
control, no inhibitor	201 $\pm$ 3 ( $n$ = 3)	2.6 $\pm$ 0.6 ( $n$ = 4)	1.3 $\pm$ 0.3
NQNO, 5 $\mu$ M	151 $\pm$ 8 ( $n$ = 3)	1.5 $\pm$ 0.1 ( $n$ = 3)	0.9 $\pm$ 0.1
DBMIB, 2 $\mu$ M	11 $\pm$ 2 ( $n$ = 3)	nd ( $n$ = 3)	—
DBMIB, 5 $\mu$ M	0.2 $\pm$ 0.4 ( $n$ = 3)	nd ( $n$ = 3)	—

<sup>a</sup> $n$  is the number of trials. "nd" indicates not determined.

**Properties of Inhibitors.** *NQNO*. *NQNO* is an  $n$ -side quinone ( $Q_n$ ) ligand of heme  $c_n$ ,<sup>1</sup> and it has been shown to inhibit oxidation of heme  $b_n$ .<sup>32–34</sup> Binding of *NQNO* to the  $b_6f$  complex in thylakoid membranes increases the amplitude of the flash-induced heme  $b_n$  reduction by a factor of 2–3 without significantly inhibiting linear electron transport or oxygen evolution. In this study, concentrations of *NQNO* that affect the amplitude of heme  $b_n$  reduction only partly inhibit linear electron transport, and *NQNO* does not increase the rate of

$O_2^{\bullet-}$  production as does addition of antimycin A to the  $bc_1$  complex (Tables 2–4 compared to Table 1). The difference in binding of  $n$ -side quinone analogue inhibitors in the  $bc_1$  and  $b_6f$  complexes resides in the multiple interactions with the amino acid environment that stabilize ligand binding at the  $Q_n$  site of the  $bc_1$  complex, whereas in the  $b_6f$  complex where heme  $c_n$  occludes access to heme  $b_n$ , the  $Q_n$  site protrudes into the intermonomer cavity, with relatively few stabilizing interactions from coordinating amino acid residues. As a result, binding of a ligand such as *NQNO* at the  $Q_n$  site is expected to be substantially weaker in the cytochrome  $b_6f$  complex than in the  $bc_1$  complex.

*DBMIB*. Halogenated quinone analogues and in particular the dibromo derivative *DBMIB*<sup>47</sup> have been described as potent inhibitors of the chloroplast cytochrome  $b_6f$  complex,<sup>45</sup> and a less efficient inhibitor of the  $bc_1$  complex from mitochondria.<sup>48</sup> *DBMIB* has been shown to bind at a position distal to the iron–sulfur binding site and also at this site.<sup>45</sup> In this study, 2  $\mu$ M *DBMIB* partially inhibits linear electron transport and  $O_2^{\bullet-}$  production of  $bc_1$  complex to approximately 20% of the uninhibited rate (Table 1). Efficient inhibition is observed for the cytochrome  $b_6f$  complex with rates of electron transport varying from undetectable to a few percent of the control (Tables 2–4), and no detectable  $O_2^{\bullet-}$  production above the background signal.

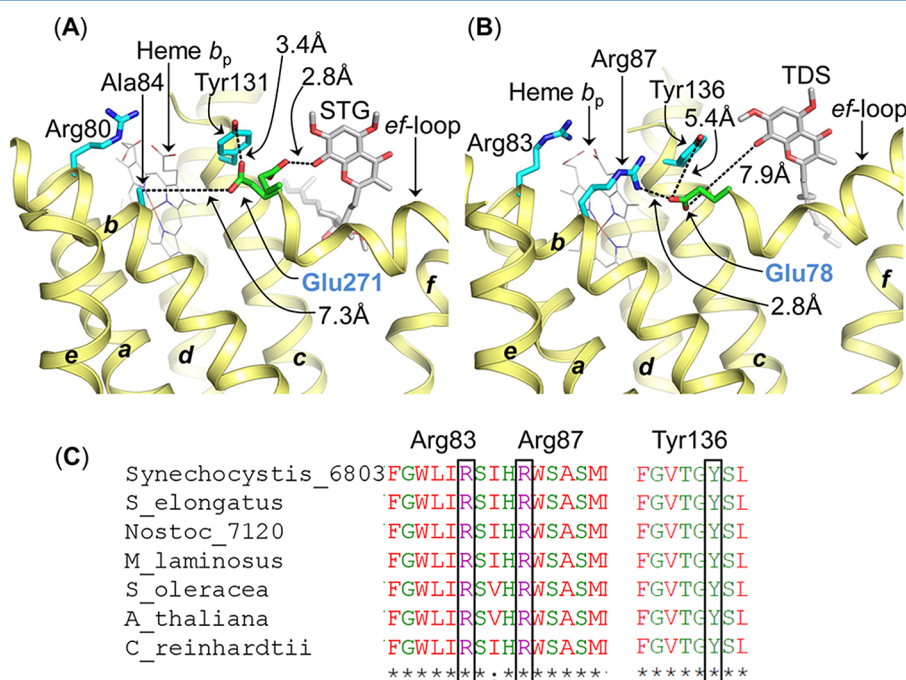


**Figure 4. Role of conserved Glu (Pro-Glu-Trp-Tyr) in semiquinone deprotonation in cytochrome  $bc$  complexes.** (A) In the  $bc_1$  complex, the Glu271 residue (green and red sticks, labeled in blue) of the PEWY sequence is found to occupy two distinct locations: quinone-proximal (PDB entry 3CX5) and heme  $b_p$ -proximal (PDB entry 1NTZ). In the heme  $b_p$ -proximal position, Glu271 interacts with Tyr131 (cytochrome  $b$  polypeptide). This structure was generated by superposition of cytochrome  $bc_1$  crystal structures (PDB entries 1NTZ and 3CX5). The STG molecule and the quinone/STG-proximal Glu271 orientation were obtained from PDB entry 3CX5. (B) In the cytochrome  $b_6f$  complex crystal structure (PDB entry 4H44), Glu78 (green and red sticks, labeled in blue) of subunit IV, homologous to Glu271 in the  $bc_1$  complex, is located in the heme  $b_p$ -proximal orientation. In this position, Glu78 interacts with Arg87 of cytochrome  $b_6$  ( $b_6f$ ), over a distance of 2.8 Å. Arg87 ( $b_6f$ ) is replaced with Ala84 (cyan sticks) in the  $bc_1$  complex. Arg83 of cytochrome  $b_6$  ( $b_6f$ ) and Arg80 of cytochrome  $b$  ( $bc_1$ ) are conserved in their locations. The quinone analogue inhibitor TDS has been inserted into the figure from PDB entry 4H13 to mark the  $Q_p$  site. Transmembrane helices a–g are labeled. The polypeptides are shown as ribbons. (C) Multiple-sequence alignment of the cytochrome  $b_6$  subunit of the cytochrome  $b_6f$  complex from prokaryotic cyanobacteria (*Synechocystis* PCC 6803, *S. elongatus* PCC 6301, *Nostoc* PCC 7120, and *M. laminosus*), a eukaryotic alga (*C. reinhardtii*), and higher plants (*A. thaliana* and *Sp. oleracea*). Arg83, Arg87 (transmembrane helix B), and Tyr136 (transmembrane helix C) are conserved in the cytochrome  $b_6$  polypeptide.

## DISCUSSION

**Origin of the Elevated Rate of Superoxide Production in the Cytochrome  $b_6f$  Complex.** *More Favorable Redox Potential of Heme  $b_p$  in the  $b_6f$  Complex.* In the literature, there are large variations in midpoint redox potentials for heme  $b_p$  in the isolated complex: (i)  $-90$  mV at pH 7,<sup>49</sup> (ii)  $-172$  mV at pH 6.5,<sup>50</sup> and (iii)  $-80$  mV at pH 6<sup>51</sup> and  $-158$  mV at pH 8.0.<sup>52</sup> For the  $bc_1$  complex, reported midpoint potentials of heme  $b_p$  are approximately  $-30$  mV in yeast and mammals,<sup>53,54</sup>  $-90$  to  $50$  mV in purple bacteria,<sup>55,56</sup> and  $0$  mV.<sup>57</sup> It is possible, but not determined by existing data, that a difference in redox potentials, e.g., a more negative potential of heme  $b_p$  in the  $b_6f$  complex, could contribute to the difference in the efficiency of superoxide formation. However, the spread of data in the literature on the heme  $b_p$  redox potentials is presently too great to allow this explanation.

*Longer Residence Time.* The higher rate of superoxide production in the  $b_6f$  complex than in the  $bc_1$  complex could arise from a longer residence time of the semiquinone in its binding niche ("Q<sub>p</sub> pocket") proximal to the iron–sulfur cluster of the Rieske iron–sulfur protein. The 10–20-fold higher rate of O<sub>2</sub><sup>•−</sup> production by the cytochrome  $b_6f$  complex compared to that of the  $bc_1$  complex (Tables 2–4 vs Table 1) implies that the rate constant in the  $b_6f$  complex for reactions iib, iii, and v is increased relative to that for reaction iv. The source of this difference can be the fact that the PQ<sub>p</sub><sup>•−</sup> generated in the  $b_6f$  complex having a lifetime in the Q<sub>p</sub> pocket longer than that of UQ<sub>p</sub><sup>•−</sup> in the  $bc_1$  complex. An identifiable structure-based cause of this longer residence time could be the partial occlusion of the Q<sub>p</sub> portal for quinone entry and exit by the phytyl chain of the unique chlorophyll *a* molecule embedded in each monomer of the complex.<sup>31</sup> This occlusion does not affect the overall rate of electron transfer through the  $b_6f$  complex, as the isolated  $b_6f$  complex supports an electron transfer rate of  $\sim 200$  electrons monomer<sup>−1</sup> s<sup>−1</sup> at room temperature,<sup>58–60</sup> which is comparable to the activity of the  $bc_1$  complex measured in ref 61 and larger than that measured in these experiments, compared to the activity of isolated  $bc_1$  complex (Tables 2 and 3 vs Table 1). Therefore, the passage of quinol through the chlorophyll-obstructed portal is not the rate-limiting step in the photosynthetic linear electron transport chain.

*Role of the Glutamate in the Conserved PEWY Sequence in Semiquinone Formation.* The neutral semiquinone species bound within the Q<sub>p</sub> site of cytochrome *bc* complexes undergoes deprotonation to form an anionic semiquinone (reaction iii), which can be a proton donor to the low-potential chain. It has been suggested that the Glu residue (Glu78 in subunit IV of the cytochrome  $b_6f$  complex and Glu271 or Glu272 in the cytochrome *b* polypeptide in the  $bc_1$  complex) of the conserved Pro-Glu-Trp-Tyr (PEWY) motif located on the p-side *ef* loop is involved in deprotonation of the neutral semiquinone to the anionic semiquinone<sup>62</sup> (Figure 4A,B), which acts as the electron donor to heme  $b_p$  (reaction iib). The motion of the Glu271 residue in the cytochrome  $bc_1$  complex during proton transfer has been demonstrated.<sup>19,63–66</sup> The Glu residue undergoes a rotation from a proton-extracting Q<sub>p</sub> niche-proximal position to a proton-releasing heme  $b_p$ -proximal position, where it interacts with the Tyr131 residue of cytochrome *b* (Figure 4A). Hence, the motion of the Glu residue constitutes an important step in the transfer of semiquinone from the Q<sub>p</sub> site. The kinetics of these reactions have recently been described.<sup>67</sup>

In the cytochrome  $b_6f$  complex, electron density for the Glu78 residue side chain, homologous to the Glu271 residue in the  $bc_1$  complex, was assigned recently in the 2.7 Å resolution crystal structure (PDB entry 4H44).<sup>20</sup> The Glu78 residue side chain is found in a heme  $b_p$ -proximal position, in which it interacts with a conserved Arg87 of the cytochrome  $b_6$  polypeptide over a short distance of 2.8 Å (Figure 4B). In this position, the Glu78 side chain does not interact with the quinone analogue inhibitor TDS (inserted into the Q<sub>p</sub> site from PDB entry 4H13). The side chain of the conserved residue Tyr136 [cytochrome  $b_6$  in the  $b_6f$  complex, transmembrane helix C (Figure 4B,C)], which replaces Tyr131 of cytochrome *b* [ $bc_1$  complex (Figure 4A)], does not interact with Glu78 in the heme  $b_p$ -proximal position. It has previously been reported that the conserved Arg87 of transmembrane helix B of the cytochrome  $b_6$  polypeptide [ $b_6f$  complex (Figure 4C)] is replaced by a small uncharged residue, such as Ala84 (or Ala83), in cytochrome *b* ( $bc_1$  complex, transmembrane helix B).<sup>68</sup> An analysis of the amino acid environment of Glu271 of cytochrome  $bc_1$  shows that the Glu271 side chain is separated from the Ala84 residue by a distance of 7.3 Å (Figure 4A). Hence, unlike the Glu78 residue in the  $b_6f$  complex that is inferred to participate in a relatively strong interaction with Arg87 in the heme  $b_p$ -proximal position, Glu271 in the  $bc_1$  complex does not interact with a basic residue from transmembrane helix B in the heme  $b_p$ -proximal position. Thus, Glu271 may be relatively free to undergo motion in the cytochrome  $bc_1$  complex, from a Q<sub>p</sub> niche-proximal position to a heme  $b_p$ -proximal position, making proton extraction and translocation from the semiquinone a relatively efficient process. On the other hand, in the  $b_6f$  complex, the motion of Glu78 is expected to be comparatively restricted because of the interaction with Arg87, thereby making proton translocation a less efficient process. As a consequence, the lifetime of the neutral semiquinone is expected to be larger within the Q<sub>p</sub> site of the cytochrome  $b_6f$  complex.

**Further Consequences of the Increased Semiquinone Retention Time.** Photosynthetic state transitions depend on the redox poise of the thylakoid membrane quinone pool.<sup>69–71</sup> The presence of reduced plastoquinone in the Q<sub>p</sub> site activates an LHCII kinase bound to the  $b_6f$  complex.<sup>72,73</sup> With regard to the application of this signaling process to cyanobacteria, although the latter possess state transitions that involve the mobility of the phycobilisomes, this does not involve kinase activation but is dependent on redox equilibria involving plastoquinone.<sup>11</sup>

**Chloroplasts as a Major Source of ROS in Plant Cells.** High irradiance and other stress conditions that affect the photosynthetic electron transport rate and create hyperoxic conditions result in a transient increase in the level of ROS in chloroplasts.<sup>9,74</sup> The major sources of ROS generated in chloroplasts are PSII (singlet oxygen) and PSI (O<sub>2</sub><sup>•−</sup>). The production of O<sub>2</sub><sup>•−</sup> by the cytochrome  $b_6f$  complex, as described in this study, has been detected by EPR spectroscopy.<sup>12</sup> Accumulated O<sub>2</sub><sup>•−</sup> can also be metabolized to another more stable form of ROS, hydrogen peroxide.<sup>11,74</sup>

The production of ROS in chloroplasts underlies oxidative damage inflicted during photosynthetic reactions,<sup>75</sup> and the redox state of photosynthetic electron transport components conveys information about environmental light conditions. Thus, chloroplasts can function as mediators of environmental signals.<sup>76</sup> Light- and stress-induced generation of ROS contributes to redox signaling inside the chloroplast and from



the organelle to the cytosol and nucleus.<sup>10,77,78</sup> ROS function in chloroplast signaling was demonstrated in relation to the regulation of dissipation and avoidance of excess excitation energy mechanisms.<sup>11</sup> The ROS generated in chloroplasts act as a retrograde signal to the nucleus for the regulation of plant responses to environmental stress and pathogen defense responses.<sup>79,80</sup> Increases in H<sub>2</sub>O<sub>2</sub> concentrations have been shown to be important for the induction of the ascorbate peroxidase gene, APX2, and for the expression of a number of genes involved in plant development and stress responses.<sup>81</sup> There is evidence that in plant disease resistance responses, ROS produced in chloroplasts interact with the signal from other intracellular and extracellular ROS sources in the modulation of the pathogen-induced hypersensitive response.<sup>82,83</sup>

## AUTHOR INFORMATION

### Corresponding Author

\*Department of Biological Sciences, Hockmeyer Hall of Structural Biology, Purdue University, West Lafayette, IN 47907. E-mail: waclab@purdue.edu. Telephone: (765) 494-4956.

### Present Addresses

<sup>†</sup>D.B.: Institute of Horticulture, Lithuanian Research Centre for Agriculture and Forestry, Babtai, Kaunas reg. Lithuania, LT 54333, Lithuania.

<sup>‡</sup>J.T.S.: Department of Chemistry and Biochemistry, University of California at San Diego, La Jolla, CA 92037.

### Author Contributions

D.B. designed superoxide experiments, purified the cytochrome *b<sub>6</sub>f* complex, performed enzymatic assays, analyzed results, and contributed to the manuscript. S.S.H. applied results to critical aspects of the crystal structure and wrote the manuscript. J.T.S. purified the cytochrome *b<sub>6</sub>f* complex, performed enzyme assays, and contributed to the analysis of the results. W.A.C. conceived the original idea, designed the experiments, analyzed the results, and wrote the manuscript.

### Author Contributions

<sup>§</sup>D.B. and S.S.H. contributed equally to this work.

### Funding

These studies were supported by National Institutes of Health Grant R01-GM038323, the Henry Koffler Distinguished Professorship (W.A.C.), a Purdue University Fellowship (S.S.H.), and infrastructure support from the Purdue University Cancer Center.

### Notes

The authors declare no competing financial interest.

## ACKNOWLEDGMENTS

We thank Prof. B. L. Trumpower for providing the yeast *bc<sub>1</sub>* complex and for helpful discussions.

## ABBREVIATIONS

ADPH, 10-acetyl-3,7-dihydroxyphenoxazine; *b<sub>p</sub>* and *b<sub>n</sub>*, *b* hemes on electrochemically positive and negative sides of the *b<sub>6</sub>f* complex, respectively; Chl *a*, chlorophyll *a*; DBMIB, 2,5-dibromo-3-methyl-6-isopropyl-*p*-benzoquinone; DDM and UDM, *n*-dodecyl and undecyl  $\beta$ -D-maltopyranoside, respectively;  $\Delta\tilde{\mu}_{H^+}$ , transmembrane proton electrochemical potential gradient; *E<sub>m7</sub>*, midpoint oxidation–reduction potential at pH 7; ISP, iron–sulfur protein; HRP, horseradish peroxidase; MOPS,

3-(*N*-morpholino)propanesulfonic acid; NQNO, 2-*n*-nonyl-4-hydroxyquinoline *N*-oxide; p-side and n-side, electrochemically positive and negative sides of the membrane and cytochrome *bc* complexes, respectively; PC, plastocyanin; PSI and PSII, photosystems I and II, respectively; *Q<sub>o</sub>*, quinone; *Q<sub>p</sub>*, p-side quinone binding site; PDB, Protein Data Bank; PQ and PQH<sub>2</sub>, plastoquinone and plastoquinol, respectively; PQ<sub>p</sub><sup>•−</sup>, plastoquinone; ROS, reactive oxygen species; O<sub>2</sub><sup>•−</sup>, superoxide; SOD, superoxide dismutase; STG, stigmatellin; TDS, tridecyl-stigmatellin; UQ and UQH<sub>2</sub>, ubiquinone and ubiquinol, respectively; UQ<sup>•−</sup>, ubisemiquinone.

## REFERENCES

- (1) Yamashita, E., Zhang, H., and Cramer, W. A. (2007) Structure of the cytochrome *b<sub>6</sub>f* complex: Quinone analogue inhibitors as ligands of heme *c<sub>n</sub>*. *J. Mol. Biol.* 370, 39–52.
- (2) Cape, J. L., Bowman, M. K., and Kramer, D. M. (2006) Understanding the cytochrome *bc* complexes by what they don't do. The Q-cycle at 30. *Trends Plant Sci.* 11, 46–55.
- (3) Cape, J. L., Bowman, M. K., and Kramer, D. M. (2007) A semiquinone intermediate generated at the *Q<sub>o</sub>* site of the cytochrome *bc<sub>1</sub>* complex: Importance for the Q-cycle and superoxide production. *Proc. Natl. Acad. Sci. U.S.A.* 104, 7887–7892.
- (4) Droese, S., and Brandt, U. (2008) The mechanism of mitochondrial superoxide production by the cytochrome *bc<sub>1</sub>* complex. *J. Biol. Chem.* 283, 21649–21654.
- (5) Forquer, I., Covian, R., Bowman, M. K., Trumpower, B., and Kramer, D. M. (2006) Similar transition states mediate the Q-cycle and superoxide production by the cytochrome *bc<sub>1</sub>* complex. *J. Biol. Chem.* 281, 38459–38465.
- (6) Lanciano, P., Khalfaoui-Hassani, B., Selamoglu, N., Ghelli, A., Rugolo, M., and Daldal, F. (2013) Molecular mechanisms of superoxide production by complex III: A bacterial versus human mitochondrial comparative case study. *Biochim. Biophys. Acta* 1827, 1332–1339.
- (7) Muller, F., Crofts, A. R., and Kramer, D. M. (2002) Multiple Q-cycle bypass reactions at the *Q<sub>o</sub>* site of the cytochrome *bc<sub>1</sub>* complex. *Biochemistry* 41, 7866–7874.
- (8) Muller, F. L., Roberts, A. G., Bowman, M. K., and Kramer, D. M. (2003) Architecture of the *Q<sub>o</sub>* site of the cytochrome *bc<sub>1</sub>* complex probed by superoxide production. *Biochemistry* 42, 6493–6499.
- (9) Mittler, R., Vanderauwera, S., Gollery, M., and Van Breusegem, F. (2004) Reactive oxygen gene network of plants. *Trends Plant Sci.* 9, 490–498.
- (10) Mittler, R., Vanderauwera, S., Suzuki, N., Miller, G., Tognetti, V. B., Vandepoele, K., Gollery, M., Shulaev, V., and Van Breusegem, F. (2011) ROS signaling: The new wave? *Trends Plant Sci.* 16, 300–309.
- (11) Mullineaux, P., and Karpinski, S. (2002) Signal transduction in response to excess light: Getting out of the chloroplast. *Curr. Opin. Plant Biol.* 5, 43–48.
- (12) Sang, M., Xie, J., Qin, X. C., Wang, W. D., Chen, X. B., Wang, K. B., Zhang, J. P., Li, L. B., and Kuang, T. Y. (2011) High-light induced superoxide radical formation in cytochrome *b<sub>6</sub>f* complex from *Bryopsis corticulans* as detected by EPR spectroscopy. *J. Photochem. Photobiol., B* 102, 177–181.
- (13) Petlicki, J., and Van de Ven, T. G. M. (1998) The equilibrium between the oxidation of hydrogen peroxide by oxygen and the dismutation of peroxyl or superoxide radicals in aqueous solutions in contact with oxygen. *J. Chem. Soc., Faraday Trans.* 94, 2763–2767.
- (14) Wood, P. M. (1988) The potential diagram for oxygen at pH 7. *Biochem. J.* 253, 287–289.
- (15) Trumpower, B. L., and Gennis, R. B. (1994) Energy transduction by cytochrome complexes in mitochondrial and bacterial respiration: The enzymology of coupling electron transfer reactions to transmembrane proton translocation. *Annu. Rev. Biochem.* 63, 675–716.

- (16) Cramer, W. A., Yamashita, E., and Hasan, S. S. (2011) The Q cycle of cytochrome *bc* complexes: A structure perspective. *Biochim. Biophys. Acta* 1807, 788–802.
- (17) Okayama, S. (1976) Redox potential of plastoquinone A in spinach chloroplasts. *Biochim. Biophys. Acta* 440, 331–336.
- (18) Trumpower, B. L. (1990) The protonmotive Q cycle. Energy transduction by coupling of proton translocation to electron transfer by the cytochrome *bc*<sub>1</sub> complex. *J. Biol. Chem.* 265, 11409–11412.
- (19) Crofts, A. R., Hong, S., Ugulava, N., Barquera, B., Gennis, R., Guergova-Kuras, M., and Berry, E. A. (1999) Pathways for proton release during ubiquinol oxidation by the *bc*<sub>1</sub> complex. *Proc. Natl. Acad. Sci. U.S.A.* 96, 10021–10026.
- (20) Hasan, S. S., Yamashita, E., Baniulis, D., and Cramer, W. A. (2013) Quinone-dependent proton transfer pathways in the photosynthetic cytochrome *b<sub>6</sub>f* complex. *Proc. Natl. Acad. Sci. U.S.A.* 110, 4297–4302.
- (21) Berry, E. A., Guergova-Kuras, M., Huang, L.-S., and Crofts, A. R. (2000) Structure and function of cytochrome *bc* complexes. *Annu. Rev. Biochem.* 69, 1005–1075.
- (22) Crofts, A. R. (2004) The cytochrome *bc*<sub>1</sub> complex: Function in the context of structure. *Annu. Rev. Physiol.* 66, 689–733.
- (23) Mitchell, P. (1975) The protonmotive Q cycle: A general formulation. *FEBS Lett.* 59, 137–139.
- (24) Joliot, P., and Joliot, A. (1988) The low-potential electron-transfer chain in the cytochrome *bf* complex. *Biochim. Biophys. Acta* 933, 319–333.
- (25) Sarewicz, M., Borek, A., Cieluch, E., Swierczek, M., and Osyczka, A. (2010) Discrimination between two possible reaction sequences that create potential risk of generation of deleterious radicals by cytochrome *bc*<sub>1</sub>. Implications for the mechanism of superoxide production. *Biochim. Biophys. Acta* 1797, 1820–1827.
- (26) Huang, L. S., Cobessi, D., Tung, E. Y., and Berry, E. A. (2005) Binding of the respiratory chain inhibitor antimycin to the mitochondrial *bc*<sub>1</sub> complex: A new crystal structure reveals an altered intramolecular hydrogen-bonding pattern. *J. Mol. Biol.* 351, 573–597.
- (27) Berry, E. A., Huang, L. S., Lee, D. W., Daldal, F., Nagai, K., and Minagawa, N. (2010) Ascochlorin is a novel, specific inhibitor of the mitochondrial cytochrome *bc*<sub>1</sub> complex. *Biochim. Biophys. Acta* 1797, 360–370.
- (28) Rottenberg, H., Covian, R., and Trumpower, B. L. (2009) Membrane potential greatly enhances superoxide generation by the cytochrome *bc*<sub>1</sub> complex reconstituted into phospholipid vesicles. *J. Biol. Chem.* 284, 19203–19210.
- (29) Yin, Y., Tso, S. C., Yu, C. A., and Yu, L. (2009) Effect of subunit IV on superoxide generation by *Rhodobacter sphaeroides* cytochrome *bc*<sub>1</sub> complex. *Biochim. Biophys. Acta* 1787, 913–919.
- (30) Kurisu, G., Zhang, H., Smith, J. L., and Cramer, W. A. (2003) Structure of the cytochrome *b<sub>6</sub>f* complex of oxygenic photosynthesis: Tuning the cavity. *Science* 302, 1009–1014.
- (31) Hasan, S. S., Yamashita, E., and Cramer, W. A. (2013) Transmembrane signaling and assembly of the cytochrome *b<sub>6</sub>f*-lipidic charge transfer complex. *Biochim. Biophys. Acta* 1827, 1295–1308.
- (32) Jones, R. W., and Whitmarsh, J. (1988) Inhibition of electron transfer and electrogenic reaction in the cytochrome *b/f* complex by 2-nonyl-4-hydroxyquinoline N-oxide (NQNO) and 2,5-dibromo-3-methyl-6-isopropyl-p-benzoquinone (DBMIB). *Biochim. Biophys. Acta* 933, 258–268.
- (33) Rich, P. R., Madgwick, S. A., and Moss, D. A. (1991) The interactions of duroquinol, DBMIB, and NQNO with the chloroplast cytochrome *bf* complex. *Biochim. Biophys. Acta* 1058, 312–328.
- (34) Furbacher, P. N., Girvin, M. E., and Cramer, W. A. (1989) On the question of interheme electron transfer in the chloroplast cytochrome *b<sub>6</sub>* *in situ*. *Biochemistry* 28, 8990–8998.
- (35) Baniulis, D., Zhang, H., Yamashita, E., Zakharova, T., Hasan, S. S., and Cramer, W. A. (2011) Purification and crystallization of the cyanobacterial cytochrome *b<sub>6</sub>f* complex. In *Methods in Molecular Biology (Photosynthesis Research Protocols)* (Carpentier, R., Ed.) pp 65–77, Humana Press Inc., Totowa, NJ.
- (36) Cramer, W. A., Yamashita, E., Baniulis, D., and Hasan, S. S. (2011) The cytochrome *b<sub>6</sub>f* complex of oxygenic photosynthesis. In *Handbook of Metalloproteins* (Messerschmidt, A., Ed.) pp 16–28, John Wiley & Sons, Chichester, U.K.
- (37) Morand, L. Z., and Krogmann, D. W. (1993) Large scale preparation of pure plastocyanin from spinach. *Biochim. Biophys. Acta* 1141, 105–106.
- (38) Massey, V. (1959) The microestimation of succinate and the extinction coefficient of cytochrome *c*. *Biochim. Biophys. Acta* 34, 255–256.
- (39) Christensen, H. E. M. (1990) A new procedure for the fast isolation and purification of plastocyanin from the cyanobacterium, *A. variabilis*. *Photosynth. Res.* 25, 72–76.
- (40) Sievers, F., Wilm, A., Dineen, D. D., Gibson, T. J., Karplus, K., Li, W., Lopez, R., McWilliam, H., Remmert, M., Soeding, J., Thompson, J. D., and Higgins, D. G. (2011) Fast scalable generation of high-quality protein multiple sequence alignments using Clustal Omega. *Mol. Syst. Biol.* 7, 539.
- (41) Goujon, M., McWilliam, H., Li, W., Valentin, F., Squizzato, S., Paern, J., and Lopez, R. (2010) A new bioinformatics analysis tools framework at EMBL-EBI. *Nucleic Acids Res.* 38, W695–W699.
- (42) Gao, X., Wen, X., Esser, L., Quinn, B., Yu, L., Yu, C. A., and Xia, D. (2003) Structural basis for the quinone reduction in the *bc*<sub>1</sub> complex: A comparative analysis of crystal structures of mitochondrial cytochrome *bc*<sub>1</sub> with bound substrate and inhibitors at the Q<sub>i</sub> site. *Biochemistry* 42, 9067–9080.
- (43) Solmaz, S. R., and Hunte, C. (2008) Structure of complex III with bound cytochrome *c* in reduced state and definition of a minimal core interface for electron transfer. *J. Biol. Chem.* 283, 17542–17549.
- (44) Sun, J., and Trumpower, B. L. (2003) Superoxide anion generation by the cytochrome *bc*<sub>1</sub> complex. *Arch. Biochem. Biophys.* 419, 198–206.
- (45) Yan, J., Kurisu, G., and Cramer, W. A. (2006) Intraprotein transfer of the quinone analogue inhibitor 2,5-dibromo-3-methyl-6-isopropyl-p-benzoquinone in the cytochrome *b<sub>6</sub>f* complex. *Proc. Natl. Acad. Sci. U.S.A.* 103, 69–74.
- (46) Yin, Y., Yang, S., Yu, L., and Yu, C. A. (2010) Reaction mechanism of superoxide generation during ubiquinol oxidation by the cytochrome *bc*<sub>1</sub> complex. *J. Biol. Chem.* 285, 17038–17045.
- (47) Bohme, H., Reimer, S., and Trebst, A. (1971) Role of plastoquinone in photosynthesis: Effect of dibromothymoquinone, an antagonist of plastoquinone, on non cyclic and cyclic electron flow systems in isolated chloroplasts. *Z. Naturforsch., B* 26, 341–352.
- (48) Gwak, S. H., Yang, F. D., Yu, L., and Yu, C. A. (1987) Phospholipid-dependent interaction between dithymoquinone and iron-sulfur protein in mitochondrial cytochrome *c* reductase. *Biochim. Biophys. Acta* 890, 319–325.
- (49) Rich, P. R., and Bendall, D. S. (1980) The redox potentials for the *b*-type cytochromes of higher plant chloroplasts. *Biochim. Biophys. Acta* 591, 153–161.
- (50) Hurt, E., and Hauska, G. (1982) Identification of the polypeptides in the cytochrome *b<sub>6</sub>f* complex from spinach chloroplasts with redox-center-carrying subunits. *J. Bioenerg. Biomembr.* 14, 405–424.
- (51) Hurt, E. C., and Hauska, G. (1983) Cytochrome *b<sub>6</sub>* from isolated cytochrome *b<sub>6</sub>f* complexes: Evidence for two spectral forms with different midpoint potentials. *FEBS Lett.* 153, 413–419.
- (52) Pierre, Y., Breyton, C., Kramer, D., and Popot, J. L. (1995) Purification and characterization of the cytochrome *b<sub>6</sub>f* complex from *Chlamydomonas reinhardtii*. *J. Biol. Chem.* 270, 29342–29349.
- (53) Wikström, M. K. F. (1973) The different cytochrome *b* components in the respiratory chain of animal mitochondria and their role in electron transport and energy conservation. *Biochim. Biophys. Acta* 301, 155–193.
- (54) T'Sai, A. L., and Palmer, G. (1983) Potentiometric studies on yeast complex III. *Biochim. Biophys. Acta* 722, 349–363.
- (55) Dutton, P. L., and Jackson, J. B. (1972) Thermodynamic and kinetic characterization of electron transfer components *in situ* in



*Rhodospseudomonas spheroides* and *Rhodospirillum rubrum*. *Eur. J. Biochem.* 30, 495–510.

(56) Crofts, A. R., Meinhardt, S. W., Jones, K. R., and Snozzi, M. (1983) The Role of the Quinone Pool in the Cyclic Electron-Transfer Chain on *Rhodospseudomonas sphaeroides*: A Modified Q-Cycle Mechanism. *Biochim. Biophys. Acta* 723, 202–218.

(57) Yun, C. H., Crofts, A. R., and Gennis, R. B. (1991) Assignment of the histidine axial ligands to the cytochrome  $b_H$  and cytochrome  $b_L$  components of the  $bc_1$  complex from *Rhodobacter sphaeroides* by site-directed mutagenesis. *Biochemistry* 30, 6747–6754.

(58) Baniulis, D., Yamashita, E., Whitelegge, J. P., Zatsman, A. I., Hendrich, M. P., Hasan, S. S., Ryan, C. M., and Cramer, W. A. (2009) Structure-function, stability, and chemical modification of the cyanobacterial cytochrome  $b_6f$  complex from *Nostoc* sp. PCC 7120. *J. Biol. Chem.* 284, 9861–9869.

(59) Zhang, H., Kurisu, G., Smith, J. L., and Cramer, W. A. (2003) A defined protein-detergent-lipid complex for crystallization of integral membrane proteins: The cytochrome  $b_6f$  complex of oxygenic photosynthesis. *Proc. Nat. Acad. Sci. U.S.A.* 100, 5160–5163.

(60) Zhang, H., Whitelegge, J. P., and Cramer, W. A. (2001) Ferredoxin:NADP<sup>+</sup> oxidoreductase is a subunit of the chloroplast cytochrome  $b_6f$  complex. *J. Biol. Chem.* 276, 38159–38165.

(61) Yu, L., Yang, S., Yin, Y., Cen, X., Zhou, F., Xia, D., and Yu, C. A. (2009) Analysis of electron transfer and superoxide generation in the cytochrome  $bc_1$  complex. *Methods Enzymol.* 456, 459–473.

(62) Zito, F., Finazzi, G., Joliot, P., and Wollman, F. A. (1998) Glu78, from the conserved PEWY sequence of subunit IV, has a key function in cytochrome  $b_6f$  turnover. *Biochemistry* 37, 10395–10403.

(63) Crofts, A. R., Barquera, B., Gennis, R. B., Kuras, R., Guergova-Kuras, M., and Berry, E. A. (1999) Mechanism of ubiquinol oxidation by the  $bc_1$  complex: Different domains of the quinol binding pocket and their role in the mechanism and binding of inhibitors. *Biochemistry* 38, 15807–15826.

(64) Hunte, C., Koepke, J., Lange, C., Rossmanith, T., and Michel, H. (2000) Structure at 2.3 Å resolution of the cytochrome  $bc_1$  complex from the yeast *Saccharomyces cerevisiae* co-crystallized with an antibody Fv fragment. *Structure* 8, 669–684.

(65) Palsdottir, H., Lojero, C. G., Trumpower, B. L., and Hunte, C. (2003) Structure of the yeast cytochrome  $bc_1$  complex with a hydroxyquinone anion  $Q_o$  site inhibitor bound. *J. Biol. Chem.* 278, 31303–31311.

(66) Izrailev, S., Crofts, A. R., Berry, E. A., and Schulten, K. (1999) Steered molecular dynamics simulation of the Rieske subunit motion in the cytochrome  $bc_1$  complex. *Biophys. J.* 77, 1753–1768.

(67) Victoria, D., Burton, R., and Crofts, A. R. (2013) Role of the -PEWY-glutamate in catalysis at the  $Q_o$ -site of the Cyt  $bc_1$  complex. *Biochim. Biophys. Acta* 1827, 365–386.

(68) Widger, W. R., Cramer, W. A., Herrmann, R. G., and Trebst, A. (1984) Sequence homology and structural similarity between the  $b$  cytochrome of mitochondrial complex III and the chloroplast  $b_6f$  complex: Position of the cytochrome  $b$  hemes in the membrane. *Proc. Natl. Acad. Sci. U.S.A.* 81, 674–678.

(69) Allen, J. F., Bennett, J., Steinback, K. E., and Arntzen, C. J. (1981) Chloroplast Protein-Phosphorylation Couples Plastoquinone Redox State to Distribution of Excitation-Energy between Photosystems. *Nature* 291, 25–29.

(70) Allen, J. F., and Horton, P. (1981) Chloroplast Protein-Phosphorylation and Chlorophyll Fluorescence Quenching-Activation by Tetramethyl-Para-Hydroquinone, an Electron-Donor to Plastoquinone. *Biochim. Biophys. Acta* 638, 290–295.

(71) Horton, P., Allen, J. F., Black, M. T., and Bennett, J. (1981) Regulation of Phosphorylation of Chloroplast Membrane Polypeptides by the Redox State of Plastoquinone. *FEBS Lett.* 125, 193–196.

(72) Lemeille, S., Willig, A., Depege-Fargeix, N., Delessert, C., Bassi, R., and Rochaix, J. D. (2009) Analysis of the chloroplast protein kinase Stt7 during state transitions. *PLoS Biol.* 7, 664–675.

(73) Rochaix, J. D. (2011) Regulation of photosynthetic electron transport. *Biochim. Biophys. Acta* 1807, 375–383.

(74) Apel, K., and Hirt, H. (2004) Reactive oxygen species: Metabolism, oxidative stress, and signal transduction. *Annu. Rev. Plant Biol.* 55, 373–399.

(75) Foyer, C. H., and Shigeoka, S. (2011) Understanding oxidative stress and antioxidant functions to enhance photosynthesis. *Plant Physiol.* 155, 93–100.

(76) Pfannschmidt, T., Schutze, K., Brost, M., and Oelmüller, R. (2001) A novel mechanism of nuclear photosynthesis gene regulation by redox signals from the chloroplast during photosystem stoichiometry adjustment. *J. Biol. Chem.* 276, 36125–36130.

(77) Fernandez, A. P., and Strand, A. (2008) Retrograde signalling and plant stress: Plastid signals initiate cellular stress responses. *Curr. Opin. Plant Biol.* 11, 509–513.

(78) Strand, A., Kleine, T., and Chory, T. (2007) Plastid-to-nucleus signaling. In *The Structure and Function of Plastids*, Advances in Photosynthesis and Respiration, pp 183–197, Springer, Berlin.

(79) Inaba, T., Yazu, F., Ito-Inaba, Y., Kakizaki, T., and Nakayama, K. (2011) Retrograde signaling pathway from plastid to nucleus. *Int. Rev. Cell Mol. Biol.* 290, 167–204.

(80) de Dios Barajas-Lopez, J., Blanco, N. E., and Strand, A. (2013) Plastid-to-nucleus communication, signals controlling the running of the plant cell. *Biochim. Biophys. Acta* 1833, 425–437.

(81) Vanderauwera, S., Zimmermann, P., Rombauts, S., Vandenabeele, S., Langebartels, C., Grissem, W., Inze, D., and Van Breusegem, F. (2005) Genome-wide analysis of hydrogen peroxide-regulated gene expression in *Arabidopsis* reveals a high light-induced transcriptional cluster involved in anthocyanin biosynthesis. *Plant Physiol.* 139, 806–821.

(82) Kangasjarvi, S., Neukermans, J., Li, S., Aro, E. M., and Noctor, G. (2012) Photosynthesis, photorespiration, and light signalling in defence responses. *J. Exp. Bot.* 63, 1619–1636.

(83) Zurbriggen, M. D., Carrillo, N., and Hajirezaei, M.-R. (2011) ROS signaling in the hypersensitive response. When, where and what for? *Plant Signaling Behav.* 5, 393–396.